known for guayulin A, but it is apparent that lipophilicity is important, both for skin penetration and possible insertion into membranes followed by alkylation of skin or serum proteins and lymphocyte recognition (*12*).

The problems that guayulin A presents in a developing guayule industry may be complicated by crossbreeding with other species of *Parthenium* to develop strains of guayule with higher rubber yields (*13*). Guayule readily undergoes interspecific hybridization with *Parthenium incanum* (mariola), a close desert relative, and with *P. tomentosum* var. *stramonium*, an arborescent species common to Sinaloa, Mexico. These two species contain sesquiterpene lactones that are cytotoxic and produce allergic skin reactions in persons initially sensitized to species belonging to the sunflower family (Asteraceae). Preliminary investigations of crosses of *P. tomentosum* var. *stramonium* with guayule indicate the presence of guayulin A and stramonin B, a cytotoxic pseudoguaianolide, in the first filial generation of the experimental hybrids.

Allergic contact dermatitis is a leading occupational health problem today in terms of the number of persons afflicted and probably also in terms of misery (*14*). Guayule-processing facilities can be planned now to minimize worker contact with resins; rubber-processing procedures can be designed to ensure removal of allergens in final products to a safe level; breeding programs can select for strains low in allergen content as well as for high rubber yield. Since widespread cultivation of guayule in marginal arid regions around the world is likely, it would be wise to initiate studies of the potency of guayule allergens on humans and of occupational dermatitis in existing guayule-processing pilot plants.

ELOY RODRIGUEZ*
GARY W. REYNOLDS
JAMES A. THOMPSON
Phytochemistry Laboratory, Department of Developmental and Cell Biology, and *Department of Ecology and Evolutionary Biology, University of California, Irvine 92717*

References and Notes

1. E. Campos, J. G. Delgado, M. A. P. Velez, E. Neavez, C. Valazquez, M. Velazquez, *Cienc. Desarrollo* **15**, 13 (1977).
2. L. M. Smith and R. P. Hughes, *Arch. Dermatol. Syphilol.* **38**, 778 (1938).
3. E. Rodriquez, W. L. Epstein, J. C. Mitchell, *Contact Dermatitis* **3**, 155 (1977).
4. Guayule plants were obtained from the Los Angeles Arboretum, Arcadia, Calif.
5. B. Magnusson and A. M. Kligman, *J. Invest. Dermatol.* **52**, 268 (1969). Sensitization to guayule resin by the procedure outlined in Magnusson and Kligman included two injections of 10 percent resin in Freund's complete adjuvant (FCA), two injections of 20 percent resin in propylene glycol, and two injections of FCA alone; each injection was 0.1 ml, given intradermally in the intersacral region on the same day. Topical application of 50 percent guayule resin in propylene glycol was made in the intersacral area 2 days after the intradermal injections and was occluded for 24 hours. Challenges were made 14 days later. All animals used in the study were female Hartley strain guinea pigs, 350 to 450 g, in groups of eight to ten. Control groups received similar injections of FCA and vehicle without guayule resin.
6. Guayulin A ^{1}H NMR (90 MHz) spectrum in $CDCl_3$: 0.98 (1H, dd, J = 11 Hz, J = 9 Hz, C-7), 1.10 (3H, s, C-12 or 13), 1.14 (3H, s, C-12 or 13), 1.57 (3H, d, J = 1.5 Hz, C-15), 1.60 (1H, dd, J = 11.5 Hz, J = 9 Hz, C-6), 1.69 (3H, d, J = 1.5 Hz, C-14), 2.1 (5H, m, C-2, 3, and 9′), 2.81 (1H, dd, J = 5.5 Hz, J = 12.5 Hz, C-9), 4.53 (1H, dd, J = 1.5 Hz, J = 11.5 Hz, C-5), 4.92 (1H, dt, J = 5.5 Hz, J = 11 Hz, C-8), 5.15 (1H, m, C-1), 6.44 (1H, d, J = 16 Hz, $-C\underline{H}=CH-C_6H_5$), 7.47 (5H, m, $-C_6H_5$), 7.68 (1H, d, J = 16 Hz, $-CH=C\underline{H}-C_6H_5$).
7. J. Romo, A. Romo de Vivar, A. Oretega y E. Draz, *Rev. Latinoam. Quim.* **2**, 332 (1970). Samples of guayulin A and B, obtained from A. Romo de Vivar, were identical to the substances we isolated from guayule. We did not detect partheniol or its cinnamate derivative.
8. G. Kelcak, in *Dermatotoxicology and Pharmacology*, F. N. Marzulli and H. Maibach, Eds. (Wiley, New York, 1977). Guinea pigs were sensitized with 5 percent guayulin A in FCA. Four 0.1-ml intradermal injections were given in the intersacral area every other day, for a total sensitizing dose of 20 mg of guayulin A. Two weeks were allowed for hypersensitivity to develop before challenges were made. Challenges consisted of 5-μl drops of compounds in serial threefold dilutions in acetone beginning at 10 percent (weight to volume) applied to a circle of bare skin 8 mm in diameter.
9. H. Baer, R. C. Watkins, A. P. Kurtz, J. S. Kurtz, J. S. Byck, C. R. Dawson, *J. Immunol.* **99**, 370 (1967).
10. G. H. N. Towers, J. C. Mitchell, E. Rodriquez, P. V. Subba Rao, F. D. Bennett, *J Sct. Ind. Res. Sect. C* **36**, 672 (1977).
11. Guayulin A was assayed by high performance liquid chromatography with detection at 254 nm.
12. The possible insertion of lipophilic contact allergens into cell membranes has been suggested by C. Benezra (Strasbourg, France), G. H. N. Towers (Vancouver, B.C.), and N. Castagnoli (University of California, San Francisco).
13. Plant-breeding experiments with guayule are currently under way at the Los Angeles Arboretum, Arcadia, Calif., under the direction of G. Hanson.
14. W. L. Epstein, H. Baer, C. R. Dawson, R. G. Khurara, *Arch. Dermatol.* **109**, 356 (1974).
15. We thank the National Science Foundation (grant PFR-7825162) and H. T. Huang for support of this investigation and W. L. Epstein and H. Maibach for help in the dermatological investigations.

3 October 1980

Metabolic Mapping of the Brain's Response to Visual Stimulation: Studies in Humans

Abstract. *These studies demonstrated increasing glucose metabolic rates in the human primary (PVC) and associative (AVC) visual cortex as the complexity of visual scenes increased. The metabolic response of the AVC increased more rapidly with scene complexity than that of the PVC, indicating the greater involvement of the higher order AVC for complex visual interpretations. Increases in local metabolic activity by as much as a factor of 2 above that of control subjects with eyes closed indicate the wide range and metabolic reserve of the visual cortex.*

Much recent understanding of the anatomical and functional makeup of the visual system has been derived from electrophysiological studies, typically through the use of single cell recordings, such as those carried out by Hubel and Wiesel, who have extensively reviewed the subject (*1*). Some studies in which electrodes have been placed intraoperatively on the cortical surface have also been performed with human subjects (*2, 3*). These and anatomical studies in animals or in humans with lesions in different parts of the visual system have delineated the highly organized structure and function as well as the clear species differences that exist in the visual system.

Scalp electrodes have been used in human electrophysiological studies to measure changes in evoked potentials of the visual cortex during visual stimulation. Although this technique is simple and safe, it has provided very little new information about the visual system because of the poor spatial resolution, difficulty in correlating the evoked potential with cortical neurophysiology, and to some degree the variability of the technique.

Cerebral blood flow, which is considered to provide an index of cerebral function, has been measured in animals to evaluate the visual system's response to stimulation (*4, 5*). Ingvar *et al.* (*6*) injected ^{133}Xe into the carotid artery to study eye movements but not the visual cortex.

Although cerebral blood flow is believed to be normally related to cerebral function, measuring local metabolic rates would provide a more direct evaluation. Human hemispheric metabolism has frequently been studied by the Kety-Schmidt method, but this technique is insensitive to changes in local cerebral function (*7*) and requires jugular vein and arterial catheterization with their associated trauma and risks. An autoradiographic technique for measuring the local cerebral metabolic rate for glucose in animals with 2-[^{14}C]deoxy-D-glucose (DG) has been developed by Sokoloff *et al.* (*8*). DG is a substrate that com-

0036-8075/81/0327-1445$00.50/0

petes with glucose for the facilitated membrane transport system and hexokinase. Its end product, DG-6-phosphate (DG6P), is not further metabolized and is essentially trapped in the cell because of its low membrane permeability. The rate of accumulation or the net accumulation of DG6P over a given time is proportional to the glycolytic rate. The autoradiographic measure of local tissue ^{14}C concentration, measurement of the arterial plasma DG and glucose concentrations, appropriate rate constants, and a tracer kinetic model developed by Sokoloff *et al.* allow the calculation of the local cerebral metabolic rate for glucose (*8*). These data are displayed as cross-sectional high-resolution images or maps of the distribution of cerebral metabolism.

The DG technique can now be applied to human subjects. Whereas ^{14}C is not detectable externally, ^{18}F—a positron-emitting radionuclide—has been incorporated into DG (*9*) to form 2-[^{18}F]fluoro-2-deoxy-D-glucose (FDG). The FDG behaves in the same manner as DG (*10, 11*). The ^{18}F tissue concentration is measured with a positron computed tomograph (*12*), which consists of a circumferential ring of detectors that measure the radiation emitted from the patient subsequent to the intravenous injection of FDG. These data are then used to mathematically reconstruct cross-sectional images of the distribution of ^{18}F tissue concentrations, allowing detailed examination of each slice, much as can be accomplished by tissue sectioning in autoradiography, and providing quantitative evaluation of metabolism in resting, stimulated, and pathological states (*10, 11, 13, 14*).

We have developed a tracer kinetic compartmental model (*11*), an extension of Sokoloff's model, that additionally accommodates the slow dephosphorylation of FDG-6-phosphate (FDG6P) by phosphatase. This reaction is not significant in autoradiography since the animal is killed at 45 minutes (*8*), but it is significant at the later time intervals of our in vivo studies. We have measured the model rate constants for FDG in humans and have found a precision of about ±5 percent (standard deviation) for glucose metabolic rate in 1.5-cm^2 regions. This method has now been integrated in our tomograph to provide a direct approach to the measurement of the local metabolic rate. The tomograph used in our work is the ECAT (EG & G–ORTEC, Inc.) (*12*). In all the studies, 5 to 10 mCi of FDG were injected intravenously, and blood was sampled from a vein of a hand heated to 44°C to produce arterialization (that is, an arteriovenous shunt); 40 to 50 minutes elapsed before imaging was initiated. Scanning times of about 30 minutes were required to image levels containing the visual cortex (typically three levels, although a total of five to six were usually imaged). Resolution in the image plane and slice thickness were about 16 and 18 mm. This procedure and the tomograph have been described (*11, 12*).

We used this technique to measure the metabolic response of the visual cortex to visual stimulations of increasing complexity. Unless otherwise stated, all subjects were studied in a controlled environment with a minimum of background noise and low-level background illumination and were dark-adapted for 15 to 20 minutes. Subjects (20 to 25 years of age) were given standard clinical examinations and latency tests of visual evoked potential, the results of which were judged to be normal.

In experiment 1, five normal volunteers were stimulated with white light (570 lux). A control study was first performed with the subjects' eyes closed and patched to provide a measure of (i) the local metabolic rate for glucose in the visual cortex that resulted from spontaneous discharge of the retinal and lateral geniculate cells and (ii) the functional baseline activity of the cortical tissue. The next day, after decay of the ^{18}F (2-

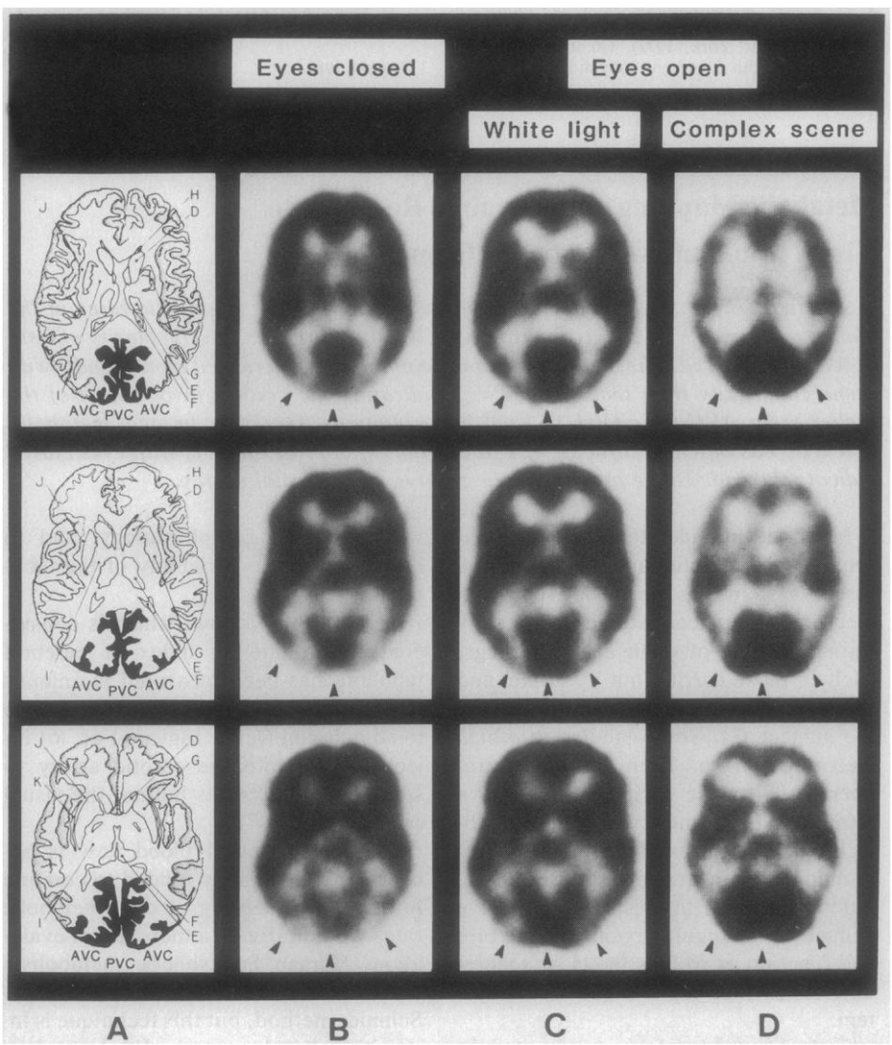

Fig. 1. (A) Sketches from actual brain slices at approximately the level of the cross-sectional tomographic images (4.4, 3.6, and 2.8 cm above the orbital-meatal plane). The blackened areas at the posterior of the brain indicate approximate location of primary (*PVC*) and associative (*AVC*) visual cortices. (B) When the eyes are closed and patched, the tissue metabolic activity is relatively low. (C) Stimulation by white light. Increasing glucose metabolic rate appears as increasing shades of gray, with black being the highest. Note the higher metabolic rate of the PVC and AVC (arrows) when the subject is being visually stimulated. The border zone between the posterior parietal cortex and the Brodmann area 19 of the AVC is also apparent when its metabolic rate is decreased in the unstimulated state. (D) Metabolic response of the visual cortex to the viewing of a complex visual scene.

hour half-life), the subjects were repositioned in the tomograph according to anatomical landmarks, aligned by use of a low-power neon laser, and stimulated visually. Stimulation was started 5 minutes before injection of FDG and continued throughout the study (Fig. 1). The average increase in glucose metabolic rate in the primary visual cortex (PVC, Brodmann area 17) and associative visual cortex (AVC, Brodmann areas 18 and 19) were bilaterally 12 and 6 percent, respectively (Fig. 2). This low metabolic response probably results from the simplicity of the visual stimulation and the fact that, in mammals and probably in humans, most of the light intensity discrimination occurs in the lateral geniculate and the superior colliculus (*15*). This hypothesis is supported by autoradiographic studies in rats stimulated with an increasing intensity of white light. A logarithmic response of the glucose metabolic rate was observed in the lateral geniculate and superior colliculus, but only a small increase was observed in the visual cortex (*16*). The small change in the AVC may also reflect the limited involvement of this higher order structure with a simple visual scene. Cooper *et al.* (*3*), using implanted electrodes and thermistors (for measuring cerebral blood flow) in the human PVC and AVC, found that only the PVC was activated during stimulation with a flickering white light, whereas both the PVC and AVC were involved in the more complex visual stimulation of reading.

In experiment 2, we increased the complexity of the visual scene with an alternating black and white checkerboard pattern (2 cycles per second), thereby adding moving edges and spatial frequency discrimination to stimulation by light intensity. Six subjects were studied, first with their eyes closed and then with the checkerboard stimulation. In these studies, the PVC and AVC showed an increased metabolic response compared with white light stimulation (Fig. 2). The increased complexity of the alternating checkerboard pattern evoked about a 2.4-fold increase in the metabolic response of the PVC, whereas the metabolic response of the higher order AVC increased by a factor of about 4.4. This greater response of the AVC may reflect the more complex visual interpretation required by the alternating checkerboard.

Three of the subjects were also tested with the alternating checkerboard pattern with one eye closed and patched. Stimulation of one eye produced a metabolic rate in the PVC about 63 percent of

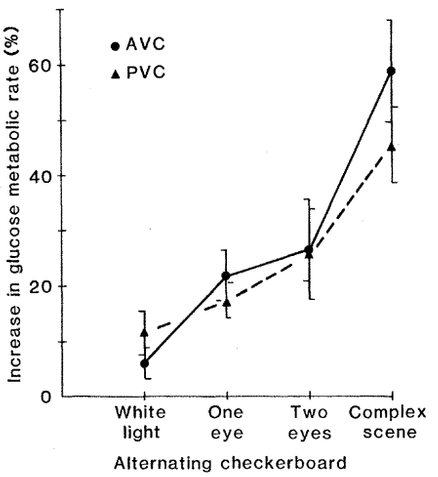

Fig. 2. Mean (± standard deviation) increase in the glucose metabolic rate of the PVC and AVC in accordance with increasing complexity of visual stimulation. Data are percentage increases above the baseline control values (with the eyes closed) of 8.40 and 6.66 mg of glucose per minute per 100 g of tissue in PVC and AVC, respectively. The metabolic response of the PVC increases by about a factor of 4, whereas the increase in the AVC is about a factor of 10.

that produced by stimulation of both eyes; no statistically significant change between binocular and monocular stimulation was noted in the AVC. Since closing one eye eliminates half the visual input to the visual cortices, one might expect the metabolic response, relative to the eyes-closed control, to be half that of the binocular stimulation. The difference between our measured result and the expected one is not likely due to spontaneous firing of precortical (retinal or geniculate) cells since the change in metabolic response of both the binocular and monocular stimulation are relative to a common baseline with the eyes closed.

A possible explanation for a greater-than-expected metabolic response in this situation might be the added demands on the visual cortex during monocular vision, altered interactions between ocular dominance columns (disinhibition), or the existence of three types of complex cells in the visual cortex (*1*). The first group of cells responds to input from the ipsilateral eye, the second to input from the contralateral eye, and a third to input from either eye. Since cells of the third group have bilateral input, the metabolic response with one eye closed should not be half the binocular response, which is consistent with our findings. DG autoradiography studies in the monkey by Kennedy *et al.* (*17*) demonstrated that the metabolic rate of the visual cortex was reduced less when one eye was patched than with unilateral enucleation, but no quantitative values were given.

Glucose metabolic rates in the PVC and AVC were symmetrical in subjects receiving monocular (left:right ratio, 1.02 ± 0.02) as well as binocular (1.03 ± 0.04) stimulation. These data confirm that each eye provides half of the input to each visual cortex in humans. In contrast, in rats and rabbits, each eye provides about 85 and 100 percent respectively, of the input to the contralateral visual cortex.

The visual stimulation was made still more complex by allowing two subjects to observe the complex visual environment in a park beside our laboratory (Fig. 1). This provided a multifaceted visual stimulation, so we could examine the metabolic requirements to process and interpret a highly complex scene and make some estimate of the metabolic reserve of the visual cortex. The metabolic response of the visual cortex was the largest we have observed from visual stimulation: about 45 percent above baseline in the PVC and 59 percent in the AVC. However, local regions of the visual cortex exhibited increases of as much as 100 percent. The larger increases in the AVC apparently reflect extensive recruitment of the AVC for the complex visual interpretations required for this visual scene. The only other studies in which we have observed such large metabolic increases were in seizure foci of patients with epilepsy (Kuhl *et al.*, *14*). This result demonstrates the large range and metabolic capacity of the visual cortex.

Similar studies as well as investigations of patients with congenital and acquired blindness, visual hallucinations, visual stimulation of patients with homonymous hemianopsia, and comparisons of the metabolic response with the visual evoked potential are the subject of a more extensive paper (*18*).

We have shown how positron computed tomography can map the distribution of local cerebral metabolic function in humans in a safe and noninvasive manner that is not possible by any other technique. These studies demonstrate that simple visual stimulation with white light produces a small but measurable metabolic response in the PVC and an even smaller response in the AVC. As the complexity of the visual scene is increased, a concomitant increase in metabolic response of the visual cortex occurs. The complex visual interpretations associated with complex visual scenes appear to progressively increase the in-

volvement of the AVC as indicated by its metabolic response (Fig. 2).

The combination of positron computed tomography to measure the concentration of radioactivity in tissue in vivo, together with the use of physiologically active compounds labeled with positron-emitting isotopes (for example, ^{11}C, ^{13}N, ^{15}O, and ^{18}F) (*19*) and tracer kinetic models allows one to measure local physiological processes in human subjects. By selecting appropriate labeled compounds and tracer kinetic models, studies of local neurotransmitters, membrane transport, blood flow, protein synthesis, and other physiologic processes are feasible.

MICHAEL E. PHELPS
DAVID E. KUHL
Division of Nuclear Medicine, Department of Radiology, UCLA School of Medicine, Los Angeles 90024, and *Laboratory of Nuclear Medicine and Radiation Biology, University of California, Los Angeles*
JOHN C. MAZZIOTTA
Department of Neurology, UCLA School of Medicine

References and Notes

1. D. H. Hubel and T. N. Wiesel, *Proc. R. Soc. London Ser. B.* **198**, 1 (1977); ———, M. P. Stoyker, *Nature (London)* **269**, 328 (1977).
2. W. Penfield and T. Rasmussen, *The Cerebral Cortex of Man* (Macmillan, New York, 1950), pp. 135–147.
3. R. Cooper, H. J. Crow, L. L. Winter, *Brain Res.* **3**, 174 (1966).
4. L. Sokoloff, in *The Regional Chemistry, Physiology and Pharmacology of the Nervous System*, S. S. Kety and J. Elkes, Eds. (Pergamon, Oxford, 1961), p. 107.
5. M. Kato, U. Hideo, P. Black, *Exp. Neurol.* **42**, 65 (1974).
6. D. H. Ingvar and N. H. Lassen, Eds., *Cerebral Function, Metabolism and Circulation* (Munksgaard, Copenhagen, 1977), p. 262–288.
7. L. Sokoloff, in *Basic Neurochemistry*, G. J. Siegel, R. W. Alberts, R. Katzman, B. W. Agronoff, Eds. (Little, Brown, Boston, 1976), p. 388–413.
8. L. Sokoloff *et al.*, *J. Neurochem.* **28**, 897 (1977).
9. T. Ido, C. N. Wan, J. S. Fowler, A. P. Wolf, *J. Org. Chem.* **42**, 2341 (1977).
10. E. M. Bessel, A. B. Foster, J. H. Westwood, *Biochem. J.* **128**, 199 (1972); M. Reivich, D. Kuhl, A. Wolf, J. Greenberg, M. Phelps, T. Ido, V. Casella, E. Hoffman, A. Alavi, L. Sokoloff, *Circ. Res.* **44**, 127 (1979); D. E. Kuhl, E. Hoffman, M. E. Phelps, A. Ricci, in *Medical Radionuclide Imaging* (International Atomic Energy Agency, Vienna, 1977), pp. 309–320; B. M. Gallagher, J. Fowler, R. R. Gutlerson, G. MacGregor, C. N. Wan, A. P. Wolf, *J. Nucl. Med.* **19**, 1154 (1978).
11. M. E. Phelps, S. C. Huang, E. J. Hoffman, C. Selin, L. Sokoloff, D. E. Kuhl, *Ann. Neurol.* **6**, 371 (1979); S. C. Huang, M. E. Phelps, E. J. Hoffman, K. Sideris, C. J. Selin, D. E. Kuhl, *Am. J. Physiol.* **238**, E69 (1980).
12. M. E. Phelps, *Sem. Nucl. Med.* **7**, 337 (1977); ———, E. J. Hoffman, S. C. Huang, D. E. Kuhl, *J. Nucl. Med.* **19**, 635 (1978).
13. D. E. Kuhl, M. E. Phelps, A. P. Kowell, E. J. Metter, C. Selin, J. Winter, *Ann. Neurol.* **8**, 47 (1980); M. Reivich, J. Greenberg, A. Alavi, D. Christman, J. Fowler, P. Hand, A. Rosenquist, W. Rintelman, A. Wolf, in *Cerebral Blood Flow and Metabolism*, F. Gotch, H. Nagai, Y. Tazaki, Eds. (Hidejima Seihanjo, Tokyo, 1979), p. 198.
14. D. E. Kuhl, J. Engel, M. E. Phelps, C. Selin, *Ann. Neurol.* **8**, 348 (1980).
15. G. F. Poggio, in *Medical Physiology*, B. V. Mountcastle, Ed. (Mosby, St. Louis, 1968), p. 1592.
16. M. Miyaoka, M. Shinohara, M. Botipps, K. D. Pettigrew, C. Kennedy, L. Sokoloff, *Acta Neurol. Scand. Suppl.* **172**, 16 (1979).
17. C. Kennedy, M. H. Des Rosiers, J. W. Jehle, M. Reivich, F. Sharpe, L. Sokoloff, *Science* **187**, 850 (1975).
18. M. E. Phelps, J. C. Mazziotta, D. E. Kuhl, M. Nuwer, J. Packwood, J. Metter, *Neurology*, in press.
19. Fluorine-18 is used as a hydrogen or hydroyl replacement because of its similar size (for example, similar steric hindrance), strong carbon-fluorine bond, and minimum effects of the differences in electronegativity. Whereas ^{18}F is used to label analogs of natural compounds, ^{11}C, ^{13}N, and ^{15}O are used as direct substitutes of these elements in natural compounds.
20. Partially supported by Department of Energy grant DEAMOS-76-SF00012 and NIH grants ROI-GM-24839-01 and PO-NS 156540-01.

7 April 1980; revised 21 October 1980

Pentobarbital: Dual Actions to Increase Brain Benzodiazepine Receptor Affinity

Abstract. *The binding of [^{3}H]diazepam to benzodiazepine receptors was studied in extensively washed membranes of rat cerebral cortex in the presence of the depressant barbiturate, pentobarbital. Pentobarbital, like the endogenous neurotransmitter γ-aminobutyric acid (GABA), increased the basal binding and also potentiated the GABA-enhanced binding of [^{3}H]diazepam to benzodiazepine receptors by increasing the apparent affinity of [^{3}H]diazepam for the benzodiazepine receptor. The concentrations of pentobarbital necessary to elicit these effects in vitro are the same as those observed after treatment with pharmacologically relevant doses, suggesting that a common neurochemical association may exist between these two types of compounds.*

Barbiturates are effective general anesthetics, sedative-hypnotics, and anticonvulsants (*1*) and share the last two therapeutic effects with the benzodiazepines. There is also compelling electrophysiological evidence to suggest that both barbiturates (*2*) and benzodiazepines (*3*) enhance chloride-dependent synaptic events mediated by γ-aminobutyric acid (GABA), a widely distributed transmitter in the central nervous system (CNS) with well-established inhibitory functions (*4*). In addition, anesthetic and sedative-hypnotic barbiturates can, like GABA, directly inhibit excitability by increasing chloride conductance; this effect is blocked by drugs that antagonize the inhibitory actions of GABA (*2*, *3*).

Benzodiazepines are believed to elicit their pharmacologic effects by interacting with a specific type of receptor that is highly concentrated in the CNS (*5*). This receptor appears to be functionally coupled to both a GABA receptor and a

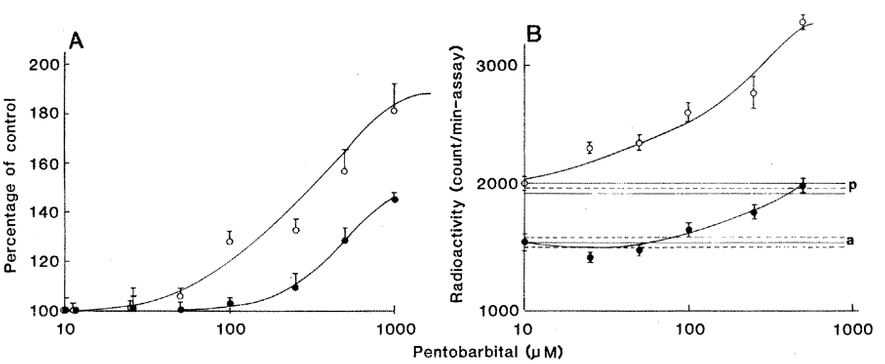

Fig. 1. Effects of pentobarbital on [^{3}H]diazepam binding to benzodiazepine receptors. (A) Pentobarbital enhancement of [^{3}H]diazepam binding in 50 m*M* tris HCl buffer (*p*H 7.4) (○) and 50 mM tris-maleate buffer (*p*H 7.4) (●). Values represent the mean ± standard error of three to eight experiments in well-washed membranes of rat cerebral cortex prepared as described in the text. The specific binding (*8*) of [^{3}H]diazepam was determined at a radioactive ligand concentration of 0.3 n*M*. The mixtures incubated contained 0.4 to 0.6 mg of protein per assay. (B) Potentiation of GABA-enhanced [^{3}H]diazepam binding by pentobarbital. Values represent the means ± standard error of triplicate determinations from a representative experiment. Symbols: [^{3}H]diazepam binding in the absence, *a*, or presence, *p*, of 0.1 μ*M* GABA; (●), [^{3}H]diazepam binding in the presence of pentobarbital (200 μ*M*) or (○) pentobarbital (200 μM) plus GABA (0.1 μ*M*). This experiment was done in tris-maleate buffer. The experiment was repeated twice with similar results and was also repeated in tris-HCl buffer, which resulted in an absolute increase in the [^{3}H]binding both in the presence and absence of the drugs. The enhanced binding in the presence of tris-HCl buffer is a result of a significant reduction in the apparent affinity of [^{3}H]diazepam (*6*, *7*). In paired experiments in which 0.3 n*M* [^{3}H]diazepam was used as a radioactive ligand, incubation of membranes in tris-maleate buffer resulted in a 50 percent reduction in basal binding (*6*, *7*, *9*).

0036-8075/81/0327-1448$00.50/0